# Multi-Channel Cross Modal Detection of Synthetic Face Images

M. Ibsen<sup>1</sup>, C. Rathgeb<sup>1</sup>, S. Marcel<sup>2</sup>, C. Busch<sup>1</sup>

- 1 Biometrics and Security Research Group, Hochschule Darmstadt, 64295 Darmstadt, Germany mathias.ibsen@h-da.de
- 2 Biometrics Security and Privacy Group, Idiap Research Institute, 1920 Martigny, Switzerland

Abstract—Synthetically generated face images have shown to be indistinguishable from real images by humans and as such can lead to a lack of trust in digital content as they can, for instance, be used to spread misinformation. Therefore, the need to develop algorithms for detecting entirely synthetic face images is apparent. Of interest are images generated by state-of-theart deep learning-based models, as these exhibit a high level of visual realism. Recent works have demonstrated that detecting such synthetic face images under realistic circumstances remains difficult as new and improved generative models are proposed with rapid speed and arbitrary image post-processing can be applied. In this work, we propose a multi-channel architecture for detecting entirely synthetic face images which analyses information both in the frequency and visible spectra using Cross Modal Focal Loss. We compare the proposed architecture with several related architectures trained using Binary Cross Entropy and show in cross-model experiments that the proposed architecture supervised using Cross Modal Focal Loss, in general, achieves most competitive performance.

# I. INTRODUCTION

Artificial intelligence (AI) has seen rapid development in the last few years, especially notably within generative models, which today are capable of synthesizing realistic digital content such as image and text which are almost indistinguishable from real data by humans [20]. Such synthetic data can have malicious use, e.g., when used for creating fake news and for performing financial fraud [15].

With today's mainly free flow of information in the digital realm, it is crucial to be able to distinguish fake digital content from pristine digital content. Of particular interest is the detection of digitally generated images. Visual stimuli have traditionally been associated with reliable information and popularized the phrase *seeing is believing*. However, face images and, in particular, the so-called Deepfakes, i.e., images and videos manipulated using advanced deep learning-based methods, has meant that this is no longer veracious. For long, a lot of focus was put on discovering images which were manipulated manually using dedicated image manipulation tools, e.g., Photoshop [21]. However, the emerging realism and availability of generative models has meant that realistic synthetic media can be generated automatically with high realism and ease [11].

It has been shown that it is possible to detect synthetic images under the assumption that the generative model is known [23]. However, detecting synthetic images across synthesis techniques is more complex, especially if both pristine

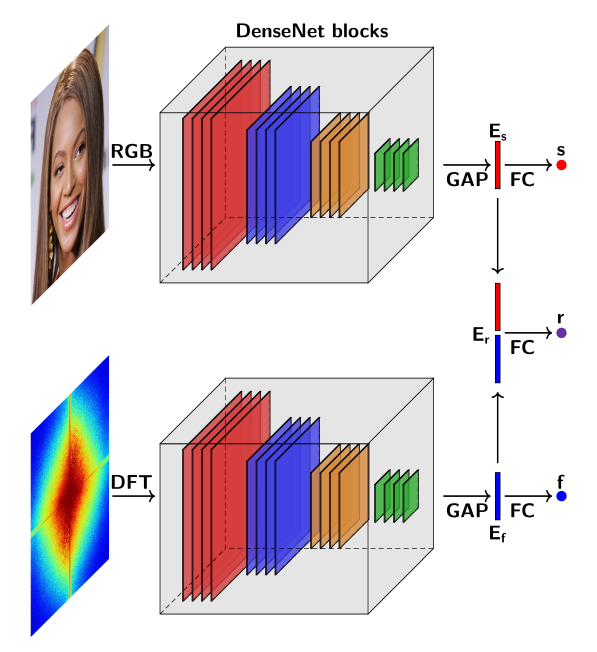


Fig. 1: Proposed multi-channel architecture for detecting synthetic face images. A RGB face image and its corresponding frequency spectrum is fed into separate network channels based on DenseNet. Global Average Pooling (GAP) is applied to the output of each channel to obtain embeddings which are concatenated into a joint representation. For each embedding a fully connected layer (FC) is added together with the Sigmoid function which results in three network heads. We propose to supervise the network using Cross Modal Focal Loss.

and fake images undergo realistic post-processing operations. Despite efforts to improve face forgery detection capabilities, recent studies show that generalization is still an ongoing and constant struggle [7]. Therefore, there is a need to continue to explore ways to improve detection performance and put forth guidelines on how to detect synthetic face images generated with unseen methods. Current studies for detecting synthetic face images usually either learn features trained directly on the RGB images or transform the images to the frequency spectrum whereafter features are extracted. Only a few works have explored the use of both frequency and RGB information for detecting synthetic face images. In this work, we propose a multi-channel architecture that uses both information from the

frequency and visible spectra to detect synthetic face images, as illustrated in figure 1. Moreover, we propose to supervise the training of the network by using the Cross Modal Focal Loss (CMFL) [6] as auxiliary learning for the separate network channels. We compare the proposed architecture to relevant single-channel and multi-channel baselines. The code for the proposed method is made available <sup>1</sup>.

This paper makes the following contributions:

- A multi-channel architecture for detecting synthetic face images using the RGB and frequency spectra
- The use of CMFL for detecting synthetic face images
- An extensive evaluation of the generalizability capability of the proposed architecture, including a comparison to related architectures and loss functions

## II. RELATED WORK

Methods for detecting synthetic face images usually rely on artefacts or statistical differences in pixel intensities or textures between pristine and fake images. Most works prior to the deep learning-based methods relied on handcrafted features, e.g., by exploiting visual artefacts such as missing reflections, lack of geometry, and differences in eye color [19] or by analyzing differences in landmark localization [24]. Nowadays, most approaches are deep learning-based and rely on large image datasets to learn discriminative features that allow distinguishing between pristine and fake images. Early works, such as [22], showed that it was possible to detect synthetic face images in the visible spectra using Convolutional Neural Networks (CNNs) when images were generated by the same model. However, they did not explore the performance on images stemming from generative models not seen during training. In [23], the authors show that by using data augmentation and training on only ProGAN-generated images, it is possible to achieve surprisingly high performance with a mean average precision (AP) higher than 90% for some training configurations when evaluated on 11 different CNNbased image generators.

Besides detecting images in the visible spectrum it has also been shown that it is possible to detect synthetic face images in the frequency domain by taking advantage of unnatural firm peaks in the frequency spectrum which, especially, can occur due to the up-sampling performed by the generative model [7]. In [26], the authors propose to detect images in the frequency spectrum instead of the spatial domain after observing that artefacts are manifested in the frequency domain of synthetic images. It has been shown, e.g., in [3], that such artefacts in the frequency spectrum can be consistent across different generative model architectures.

While multi-channel methods have already been proposed for detecting synthetic and tampered face images, they are typically proposed for other types of digital manipulations, e.g., identity swaps [18], [8] or the learning scenario is different as they either consider score-level [2], [27] or feature-level [4] fusion of the branches. These learning scenarios differ

<sup>1</sup>https://github.com/dasec/Multi-Channel-Cross-Modal-Detection-of-Synthetic-Face-Images

from the proposed framework, which solves the task using CMFL for supervision of the individual branches and Binary Cross Entropy (BCE) for the joint architecture head, as further explained in the subsequent section.

#### III. PROPOSED METHOD

As mentioned, both the spatial and frequency domains have shown to be helpful in detecting synthetic face images. However, while the two spectra convey the same underlying data, it represents different views of the data, which can be useful for detection under different circumstances. Therefore, the proposed solution is a multi-channel CNN with separate channels for the RGB and frequency domain. To supervise this network, CMFL is used [6].

## A. Architecture

The architecture of the multi-channel network is shown in figure 1. As seen, the network consists of two separate network branches; one branch based on the RGB input image and another branch based on DFT of each colour channel. Each branch consists of the first eight blocks from the DenseNet161 architecture [9] initialized using pretrained weights learned on the ImageNet dataset. After each branch, global average pooling is applied to obtain a 384-dimensional embedding layer which are concattenated to form a joint embedding for the entire network. A fully connected layer plus the Sigmoid activation function is added on top of each embedding layer to form the different heads of the architecture which is required by the CMFL loss function [6].

## B. Cross Modal Focal Loss

CMFL is based on Focal Loss [17] and was first introduced in [6] for presentation attack detection (PAD). The motivation to use CMFL for detecting synthetic face images is that in cases where one channel classifies a sample with high confidence, the loss contribution of the other channel can be reduced. The assumption is that this is useful for detecting synthetic face images as sometimes artefacts manifest in the RGB domain, and other times, it is easier to detect synthetic images in the frequency domain. Hence, if it is possible to detect synthetic images using one channel, we do not want the other channel to penalize the model.

To introduce the used loss functions we start by defining cross entropy (CE) for binary classification which can be expressed as:

$$CE(p,y) = \begin{cases} -\log(p) & \text{if } y = 1\\ -\log(1-p) & \text{otherwise} \end{cases} \tag{1}$$

where y=1, in our case, denotes a pristine image and y=0 denotes a synthetic image and where p is the probability of the class. The probability of a target class,  $p_t$  can be simplied as:

$$p_t = \begin{cases} p & \text{if } y = 1\\ 1 - p & \text{otherwise} \end{cases} \tag{2}$$

hence we can now rewrite equation 1 as:  $CE(p, y) = CE(p_t) = -\log(p_t)$ . Focal loss can then be expressed as follows:

$$FL(p_t) = -\alpha_t (1 - p_t)^{\gamma} \log(p_t) \tag{3}$$

which is similar to the rewritten CE loss, but where  $(1-p_t)^{\gamma}$  acts as a modulating factor. Here,  $\gamma \geq 0$  acts as a tune-able focusing parameter and  $\alpha$  is a weighing term added to each class. The purpose of the modulating term introduced in FL is to focus the learning more on difficult samples.

The idea of CMFL is to extend this to a multi-channel network architecture with two separate input branches. Consider figure 1 where spatial (RGB) and frequency (DFT) information is given to two separate network channels, in our case DenseNet blocks. Furthermore let  $E_s$  and  $E_f$  be the embeddings obtained from computing the forward pass for the spatial and frequency domains, respectively. We can then compute  $E_r$  to be a joint representation of  $E_s$  and  $E_f$  such that we have three output embeddings, one for each channel and a combined embedding. A separate model head is then added to each embedding by adding a single fully connected dense layer followed by a Sigmoid layer after each embedding layer (see figure 1). The output probabilities of each of these heads can then be denoted as s, f, r where s and f are the probabilities of each of the branches separately and r is the probability for the joint architecture head. Given this notation, CMFL is defined as given in equation 4.

$$CMFL_{s_t, f_t} = -\alpha_t (1 - w(s_t, f_t))^{\gamma} \log(s_t) \tag{4}$$

Where  $w(s_t, f_t)$  is dependent on the probabilities given of the separate channels as expressed in equation 5 and where  $\alpha$  and  $\gamma$  are the coefficients from FL.

$$w(s_t, f_t) = f_t \frac{2s_t f_t}{s_t + f_t}$$
 (5)

For the final loss, CMFL is used as auxiliary supervision of the individual branches combined with CE for the joint architecture head. The final loss then becomes:

$$\mathcal{L} = (1 - \lambda)\mathcal{L}_{CE(r_t)} + \lambda(\mathcal{L}_{CMFL_{s_t, f_t}} + \mathcal{L}_{CMFL_{f_t, s_t}}) \quad (6)$$

where  $\lambda$  is a changeable coefficient.

## IV. EXPERIMENTAL SETUP

## A. Data

To evaluate the multi-channel architecture and loss functions, we use pristine images from the Flickr-Faces-HQ dataset (FFHQ) [1] and synthetic images from StyleGAN2 [14], StyleGAN3 [13] and SWAGAN [5]. Each of the generative models has been trained on FFHQ; for SWAGAN the model from [12] is used. For each model, 50,000 images were generated using seeds 0-49,999 with a truncation factor of 1. Examples of pristine and synthetic data are given in figure 2.

Figure 3 shows an analysis of the average frequency spectra for each used dataset computed over 1,000 randomly sampled

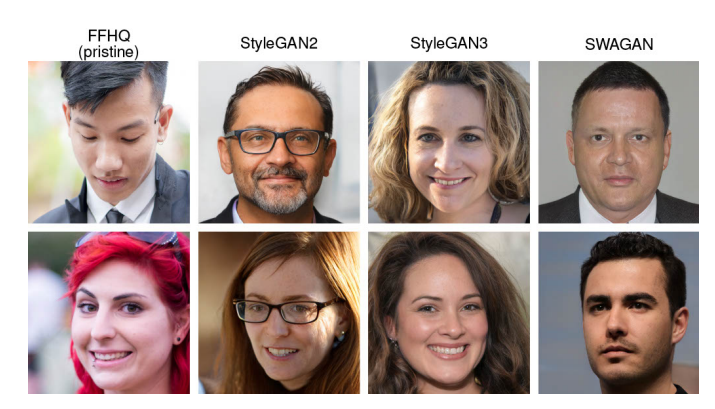


Fig. 2: Examples of pristine and synthetic images from the different used generative models.

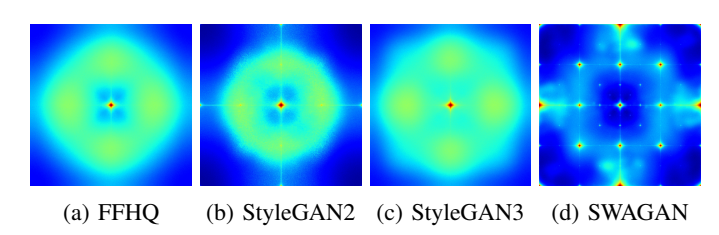


Fig. 3: Anylysis of the frequency spectra for FFHQ (pristine) and each of the generative models.

images from each dataset. To provide a more clear visualization we performed a high-pass filtering over the image by first applying a Median Blur filter to the image and then subtracting it from the input image [23]. We then perform a DFT separately on each RGB input channel (see section IV-B) and average the result over all randomly sampled images of the dataset. The averaged frequency spectra show some differences between the pristine input data and the data from the generative models, most notably for SWAGAN where clear periodic patterns can be observed.

## B. Preprocessing

In the preprocessing phase, the images are aligned and cropped to resolution  $224 \times 224$  and the DFT of each image is computed:

**Face Alignment** As this study aims to detect synthetic facial images, and i.e., not artefacts that might appear in the background of a synthetic image, a face is detected in each input image whereafter it is cropped out and the eyes aligned using the MTCNN [25] algorithm. The resulting images are of resolution 224×224 pixels and cropped to the face region.

Frequency Domain Transformation To transform an RGB image into the frequency spectrum we follow the approach in [26] and normalize the input pixels to the range [0, 1] whereafter we perform DFT for each of the 3 colour channels and obtain corresponding channels in the frequency spectrum. Thereafter, the logarithmic spectrum is computed and normalized to the range [-1, 1]. Lastly, we shift the low frequency components to the center of

the spectrum. The resulting 3D array is transformed to a tensor and given as input to the classifiers. Examples of images and their corresponding spectra is given in figure 4.

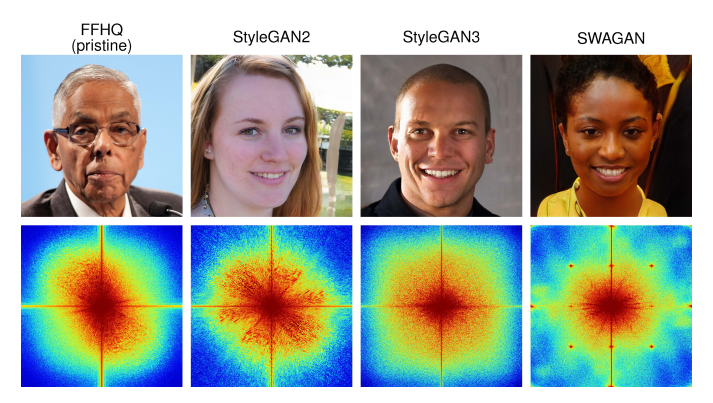


Fig. 4: Examples of pristine and synthetic images and their corresponding Fourier spectrum.

## C. Models

In this paper the performance of the proposed architecture using CMFL is compared to several related models trained using BCE. Specifically, the following models are evaluated:

**Dual-channel CMFL** This approach is based on the proposed architecture and CMFL loss function described in section III. Following [6], we set  $\gamma=3$  (equation 4) and  $\lambda=0.5$  (equation 6).

**Dual-channel BCE** This approach has the same architecture as proposed in section III, i.e., it has a separate RGB and DFT network branch, however the entire network is supervised using only the BCE loss.

One-channel RGB This approach corresponds to the singlechannel equivalent of the proposed network architecture based on only an RGB input image and where the entire network is supervised by BCE.

**One-channel DFT** This approach is similar to the *One-channel RGB* approach but operates on the computed frequency spectra of the aligned input face image instead of on the RGB image.

**Fusion (RGB + DFT)** In this model, we perform a score level fusion by computing the average between the output scores of the RGB and DFT single-channel networks.

## D. Training Details

For training, a learning rate of  $1 \cdot 10^{-4}$  is used with a weight decay of  $1 \cdot 10^{-5}$ . The DenseNet blocks are initialized using pre-trained weights from ImageNet and fine-tuned for 25 epochs using a batch size of 128, horizontal flips with probability 0.5, cross-validation, and the Adam optimizer [16]. The best model for each experiment on the validation set is saved and used during the evaluation. All models have been trained using NVIDIA A100 Tensor Core GPUs.

#### E. Metrics

To evaluate the performance of the different detection models, we show ROC curves and the following commonly used metrics:

ROC curve A Receiver Operating Characteristic (ROC) curve shows the performance of a binary classification model in terms of the True Positive Rate (TPR) and False Positive Rate (FPR) at different operating points of the system.

**AUC** The area under the curve (AUC) measures the area under a ROC curve and ranges from 0 to 1 where 1 indicates a perfect classifier and 0.5 represents random guessing.

**D-EER** Following [10], The Detection Equal Error Rate (D-EER) are the rate for a binary classification task where the error rates of the two classes are equal.

## F. Experiments

To test the different models, two protocols are proposed:

**Protocol I** In this protocol, the last 20,000 images of FFHQ are reserved for evaluation, whereas the remaining 35,000 and 15,000 images are reserved for training and validation, respectively. The generative models are evaluated following a leave-one-out protocol where a single model is used for training and validation in each iteration, and the remaining models are used for evaluation. In this protocol, no augmentation other than horizontal flipping at probability 0.5 is applied

**Protocol II** This protocol is an extension of the first protocol where Gaussian blurring and JPEG compression are applied during training. Specifically, a Gaussian blurring is applied with a  $\sigma$  sampled continuously in the range [0,2], and JPEG compression is performed with a quality factor sampled discretely from: [60,70,80,90,100]. Two types of evaluations are performed; one without any augmentation and one with augmentation. During evaluation, the same augmentation is applied per image across all the experiments to make the comparisons fair.

The purpose of these protocols is to evaluate the models under the difficult scenario where the generative model used to generate the synthetic data is unseen during training. We focus on this scenario as it has been shown that learning to detect synthetic images from a known generative model is relatively easy and usually results in a high detection performance. As the purpose of this paper is to investigate the feasibility of the proposed architecture, we focus the experiments on comparing the results to related architectures trained on the same data and which utilize similar pre-processing. The code is made available to allow comparison and inclusion in benchmarks which specifically aims at comparing state-of-the-art methods for detecting synthetic face images.

## V. RESULTS

In this section, we analyze the results for the two training and evaluation protocols. Table I shows the AUC and D-EER

TABLE I: AUC and D-EER in % for the different models and evaluation protocols. The highlighted numbers indicate the best performance (AUC or D-EER) observed across all five models for a specific train and test partition.

Model	Test Protocol	StyleGAN2				StyleGAN3				SWAGAN			
		StyleGAN3		SWAGAN		StyleGAN2		SWAGAN		StyleGAN2		StyleGAN3	
		AUC	D-EER	AUC	D-EER	AUC	D-EER	AUC	D-EER	AUC	D-EER	AUC	D-EER
	Protocol I	0.881	20.04	0.975	8.29	0.925	15.42	0.941	13.41	0.967	9.40	0.809	26.74
One-channel RGB	Protocol II (no aug.)	0.763	30.84	0.905	17.79	0.868	21.53	0.930	14.90	0.897	18.57	0.837	24.24
	Protocol II (with aug.)	0.736	32.90	0.874	21.03	0.844	23.58	0.906	17.51	0.877	20.64	0.817	26.12
One-channel DFT	Protocol I	0.787	28.29	0.855	22.40	0.925	15.32	0.418	56.19	0.482	51.79	0.479	51.95
	Protocol II (no aug.)	0.565	45.64	0.758	31.21	0.511	49.72	0.677	37.47	0.436	54.65	0.531	47.92
	Protocol II (with aug.)	0.544	47.03	0.652	39.71	0.531	48.03	0.586	43.63	0.522	48.26	0.523	48.68
Fusion (RGB + DFT)	Protocol I	0.895	18.52	0.972	8.66	0.942	13.57	0.682	36.63	0.934	13.49	0.713	34.96
	Protocol II (no aug.)	0.617	42.51	0.845	24.65	0.601	44.29	0.793	29.61	0.569	46.22	0.605	43.32
	Protocol II (with aug.)	0.608	43.21	0.774	30.57	0.622	42.49	0.725	34.61	0.599	43.81	0.575	45.57
Dual-channel BCE	Protocol I	0.908	17.48	0.978	7.51	0.982	6.76	0.951	12.01	0.953	11.21	0.722	33.75
	Protocol II (no aug.)	0.793	28.10	0.920	16.14	0.883	19.90	0.942	13.11	0.900	18.44	0.858	22.61
	Protocol II (with aug.)	0.768	30.04	0.891	19.34	0.854	22.66	0.917	16.33	0.873	21.02	0.832	24.87
Dual-channel CMFL	Protocol I	0.916	16.47	0.992	4.45	0.984	6.38	0.899	18.28	0.952	11.59	0.693	35.87
	Protocol II (no aug.)	0.784	28.86	0.923	15.65	0.894	18.96	0.947	12.60	0.909	17.23	0.864	21.85
	Protocol II (with aug.)	0.761	30.88	0.898	18.38	0.867	21.61	0.923	15.75	0.882	20.22	0.838	24.21

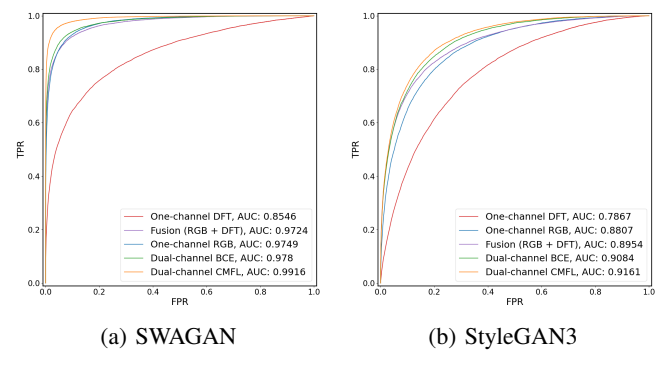


Fig. 5: ROC curves for protocol I when training on StyleGAN2

for all protocols and models. Furthermore, we highlight the results for protocol I and protocol II when training on FFHQ and StyleGAN2 using ROC curves.

As seen in table I the dual-channel approaches performs best across most test protocols and training scenarios. Furthermore, and as expected, it is easier to detect images across all models when the images are not augmented or blurred during evaluation. Hence for protocol I we observe that the best model achieves AUC > 0.90 across almost all experiments with the exception being when trained on SWAGAN and evaluated on StyleGAN3 where the best model achieves a AUC of  $\approx 0.81$ . Looking at the ROC-curve for protocol I in figure 5 when training on StyleGAN2 and evaluating on StyleGAN3 and SWAGAN, we can see that the proposed architecture with CMFL is the best model. For protocol II, shown in figure 6, we can observe that the proposed architecture using CMFL is better when evaluated on SWAGAN but that the proposed architecture with BCE is slightly better when evaluated on StyleGAN3. Looking accross all the experiments, we can see that using BCE and CMFL, in general, is quite similar but that using CMFL is better in most cases. Another finding is that DFT is not always capable of generalizing to unseen models. This is, especially, notable for protocol II when training and evaluating with realistic post-processing operations. Interestingly, poor performance for the one-channel DFT model is, especially, observed when training on SWAGAN and evaluating on StyleGAN2 and StyleGAN3 where the performance is close to random. This performance is most likely due to the SWAGAN images being easy to detect in the frequency domain due to clear artefacts (see figure 3) which are not as heavily present in the images generated by the StyleGAN models. Despite this, we can observe that even in cases where the DFT approach performs poor, the dual-channel approaches are still capable of achieving good performance due to the RGB channel which in general is capable of achieving high detection performance. Nevertheless, we can observe that the dual-channel approaches achieve superior performance to both the single-channel DFT and RGB approaches. Additionally, the results show that it is better to train the two channels jointly rather than doing a simple score fusion between the two singlechannel models. Furthermore, we can observe that in cases where both the RGB and DFT single-channel approaches have good performance, i.e., both have an AUC > 0.70, supervising the network using CMFL achieves the best performance. This indicates that CMFL can generalize better in cases where discriminative information is present in both domains.

## VI. CONCLUSION

In this work, we proposed a two-channel neural network architecture for detecting synthetic face images with one channel using information from the visible spectrum (RGB) and the other from the frequency spectrum computed separately for each colour channel using Discrete Fourier Transform. Furthermore, we proposed to supervise the network using Cross Modal Focal Loss which is capable of better modulating individual channel contribution. We evaluated the architecture on three popular generative models and compared the performance to single-channel architectures and to the same architecture supervised fully using Binary Cross Entropy. Through cross-model experiments we showed that the proposed archi-

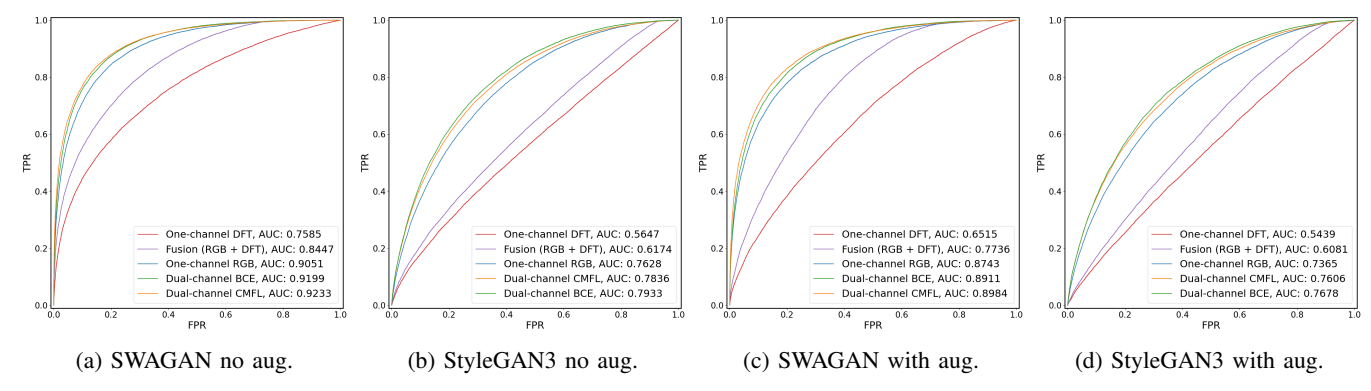


Fig. 6: ROC curves for protocol II when training on StyleGAN2.

tecture using Cross Modal Focal Loss, generally, outperformed the other models, especially in cases where images were detectable in both the visible and frequency spectra. Our studies emphasize the need to continue to understand and explore how novel loss functions can be integrated and used to detect synthetic face images and to explore the performance of detection models in challenging and realistic scenarios.

## VII. ACKNOWLEDGEMENT

This research work has been partially funded by the German Federal Ministry of Education and Research and the Hessian Ministry of Higher Education, Research, Science and the Arts within their joint support of the National Research Center for Applied Cybersecurity ATHENE and the European Union's Horizon 2020 research and innovation programme under the Marie Skłodowska-Curie grant agreement No. 860813 - TReSPAsS-ETN. Additionally, the authors would like to thank Anjith George for helpful discussions.

## REFERENCES

- Flickr-Faces-HQ Dataset (FFHQ). https://github.com/NVlabs/ffhq-dataset. Last accessed: 2023-11-28.
- [2] Z. Chen and H. Yang. Manipulated face detector: Joint spatial and frequency domain attention network. arXiv e-prints, page arXiv:2005.02958v1, 05 2020.
- [3] J. Frank, T. Eisenhofer, L. Schönherr, A. Fischer, et al. Leveraging frequency analysis for deep fake image recognition. In 37th Int'l Conf. on Machine Learning (ICML), 2020.
- [4] Y. Fu, T. Sun, X. Jiang, K. Xu, and P. He. Robust GAN-face detection based on dual-channel CNN network. In *Int'l Congress on Image and Signal Processing, BioMedical Engineering and Informatics (CISP-BMEI)*, pages 1–5, 2019.
  [5] R. Gal, D. C. Hochberg, A. Bermano, and D. Cohen-Or. SWAGAN:
- [5] R. Gal, D. C. Hochberg, A. Bermano, and D. Cohen-Or. SWAGAN: A style-based wavelet-driven generative model. ACM Trans. Graph., 40(4), jul 2021.
- [6] A. George and S. Marcel. Cross modal focal loss for RGBD face antispoofing. In 2021 IEEE/CVF Conf. on Computer Vision and Pattern Recognition (CVPR), pages 7878–7887, 2021.
- [7] D. Gragnaniello, F. Marra, and L. Verdoliva. Detection of AI-generated synthetic faces. In *Handbook of Digital Face Manipulation and De*tection: From DeepFakes to Morphing Attacks, Advances in Computer Vision and Pattern Recognition, pages 191–212. Springer Verlag, 2022.
- [8] H.-W. Hsu and J.-J. Ding. Deepfake algorithm using multiple noise modalities with two-branch prediction network. In Asia-Pacific Signal and Information Processing Association Annual Summit and Conference (APSIPA ASC), pages 1662–1669, 2021.
- [9] G. Huang, Z. Liu, L. V. D. Maaten, and K. Q. Weinberger. Densely connected convolutional networks. In *Conf. on Computer Vision and Pattern Recognition (CVPR)*, pages 2261–2269, 2017.

- [10] ISO/IEC JTC1 SC37 Biometrics. ISO/IEC 30107-3. Information Technology Biometric presentation attack detection Part 3: Testing and Reporting. International Organization for Standardization, 2023.
- [11] I. Joshi, M. Grimmer, C. Rathgeb, C. Busch, F. Bremond, and A. Dantcheva. Synthetic data in human analysis: A survey. arXiv e-prints, page arXiv:2208.09191, 08 2022.
  [12] W. Kabbani, M. Grimmer, and C. Busch. EGAIN: Extended GAn IN-
- [12] W. Kabbani, M. Grimmer, and C. Busch. EGAIN: Extended GAn INversion. In 10th European Workshop on Visual Information Processing (EUVIP), pages 1–6, 2022.
  [13] T. Karras, M. Aittala, S. Laine, E. Härkönen, et al. Alias-free generative
- [13] T. Karras, M. Aittala, S. Laine, E. Härkönen, et al. Alias-free generative adversarial networks. In *Advances in Neural Information Processing* Systems, volume 34, pages 852–863, 2021.
- [14] T. Karras, S. Laine, M. Aittala, J. Hellsten, et al. Analyzing and improving the image quality of StyleGAN. In *IEEE/CVF Conf. on Computer Vision and Pattern Recognition (CVPR)*, pages 8107–8116, 2020.
- [15] J. Kietzmann, L. W. Lee, I. P. McCarthy, and T. C. Kietzmann. Deepfakes: Trick or treat? *Business Horizons*, 63(2):135–146, 2020.
- [16] D. P. Kingma and J. Ba. Adam: A method for stochastic optimization. In *Int'l Conf. on Learning Representations (ICLR)*, 2015.
- [17] T.-Y. Lin, P. Goyal, R. Girshick, K. He, and P. Dollár. Focal loss for dense object detection. In *Int'l Conf. on Computer Vision (ICCV)*, pages 2999–3007, 2017.
- [18] I. Masi, A. Killekar, R. M. Mascarenhas, S. P. Gurudatt, and W. AbdAlmageed. Two-branch recurrent network for isolating deepfakes in videos. In *European Conference on Computer Vision (ECCV)*, pages 667–684, 2020.
- [19] F. Matern, C. Riess, and M. Stamminger. Exploiting visual artifacts to expose deepfakes and face manipulations. In *IEEE Winter Applications* of Computer Vision Workshops (WACVW), pages 83–92, 2019.
- [20] S. J. Nightingale and H. Farid. AI-synthesized faces are indistinguishable from real faces and more trustworthy. *Proceedings of the National Academy of Sciences*, 119(8):e2120481119, 2022.
- [21] C. Rathgeb, A. Dantcheva, and C. Busch. Impact and detection of facial beautification in face recognition: An overview. *IEEE Access*, 2019.
- [22] A. Rössler, D. Cozzolino, L. Verdoliva, C. Riess, et al. Faceforensics++: Learning to detect manipulated facial images. In *Intl. Conf. of Computer Vision (ICCV'19)*, 2019.
- [23] S.-Y. Wang, O. Wang, R. Zhang, A. Owens, and A. A. Efros. CNN-generated images are surprisingly easy to spot... for now. In *IEEE/CVF Conf. on Computer Vision and Pattern Recognition (CVPR)*, pages 8692–8701, 2020.
- [24] X. Yang, Y. Li, H. Qi, and S. Lyu. Exposing GAN-synthesized faces using landmark locations. In ACM Workshop on Information Hiding and Multimedia Security, pages 113—118, 2019.
- [25] K. Zhang, Z. Zhang, Z. Li, and Y. Qiao. Joint Face Detection and Alignment Using Multitask Cascaded Convolutional Networks. *IEEE Signal Processing Letters*, 23(10):1499–1503, 2016.
- [26] X. Zhang, S. Karaman, and S.-F. Chang. Detecting and simulating artifacts in GAN fake images. In *IEEE Int'l Workshop on Information Forensics and Security (WIFS)*, pages 1–6, 2019.
- [27] P. Zhou, X. Han, V. I. Morariu., and L. S. Davis. Two-stream neural networks for tampered face detection. In *Conf. on Computer Vision and Pattern Recognition Workshops (CVPRW)*, pages 1831–1839, 2017.